



# White Matter Structural Brain Connectivity of Young Healthy Individuals With High Trait Anxiety

Chunlan Yang<sup>1</sup>, Yining Zhang<sup>1</sup>, Min Lu<sup>1\*</sup>, Jiechuan Ren<sup>2</sup> and Zhimei Li<sup>2</sup>

<sup>1</sup> College of Life Science and Bioengineering, Beijing University of Technology, Beijing, China, <sup>2</sup> Beijing Tiantan Hospital, Capital Medical University, Beijing, China

**Background:** Although functional brain connectivity in anxiety-related disorders has been studied, brain connectivity in non-clinical populations with high trait anxiety has been rarely reported. Whether structural brain connectivity changes in young healthy individuals with high trait anxiety remains unknown.

**Methods:** Thirty-eight young healthy individuals with high anxiety levels and 34 healthy subjects with low anxiety levels who were matched by age, gender, and educational level were recruited. Diffusion tensor images were acquired to analyze white matter connectivity. A two-sample *t*-test was used for group comparison of weighted networks and graph properties.

**Results:** Different connections were detected in fractional anisotropy- and fiber number-weighted networks. These connections were widely distributed in various regions, where relative significance was located in the inter-hemispheric frontal lobe, the frontal-limbic lobe in the right intra-hemisphere, and the frontal-temporal lobe in the ipsilateral hemisphere. However, no significant difference was found in fiber length-weighted network and in graph properties among the three networks.

**Conclusions:** The structural connectivity of white matter may be a vulnerability marker. Hence, healthy individuals with high trait anxiety levels are susceptible to anxiety-related psychopathology. The findings may help elucidate the pathological mechanism of anxiety and establish interventions for populations susceptible to anxiety disorders.

**Keywords:** high anxiety populations, diffusion tensor imaging, white matter, structural network, connectivity, young healthy individuals

## INTRODUCTION

An increasing number of young people feel large pressure caused by the fast-paced life in our modern society. The morbidity of anxiety-related disorders has increased in recent years. Trait anxiety refers to the general traits or personality and is manifested as persistent worry and instability. Anxiety is disruptive to daily life, and long-term anxiety significantly increases the risks of developing anxiety-related disorders. We supposed that young healthy individuals with high trait anxiety level may be susceptible to anxiety-related disorders (1, 2).

The analysis of brain connectivity through graph theory and magnetic resonance imaging (MRI) has become popular in research of nervous system diseases. Previous studies demonstrated

## OPEN ACCESS

### Edited by:

Jan Kassubek,  
University of Ulm, Germany

### Reviewed by:

Costanza Gianni,  
Sapienza University of Rome, Italy  
Salem Hannoun,  
American University of  
Beirut, Lebanon

### \*Correspondence:

Min Lu  
minlu1995@163.com

### Specialty section:

This article was submitted to  
Applied Neuroimaging,  
a section of the journal  
Frontiers in Neurology

**Received:** 16 September 2019

**Accepted:** 30 December 2019

**Published:** 13 February 2020

### Citation:

Yang C, Zhang Y, Lu M, Ren J and  
Li Z (2020) White Matter Structural  
Brain Connectivity of Young Healthy  
Individuals With High Trait Anxiety.  
*Front. Neurol.* 10:1421.  
doi: 10.3389/fneur.2019.01421

abnormalities in brain connectivity among anxious patients. Zhu et al. found that changes in “small-world” properties in resting-state functional MRI (fMRI) are prominent among people with social anxiety disorders (3). Pacheco-Unguetti et al. found that trait anxiety is related to deficiencies in the executive control network, and attention-executive control function is impaired in adults with generalized anxiety disorder (4). Liao et al. found increased functional connectivity of the right posterior inferior temporal gyrus to the left inferior occipital gyrus, the right parahippocampal/hippocampal gyrus to the left middle temporal gyrus, and enhanced structural connectivity located in the genu of the corpus callosum among people with social anxiety disorders (5). Baur et al. found that the anterior insula and basolateral amygdala constitute a network markedly linked to anxiety (6).

In addition to an analysis using fMRI, electroencephalography (EEG) is used to detect abnormal connections in patients with anxiety disorders even at a rest state (7). However, T1-weighted imaging and diffusion tensor imaging (DTI) have been rarely used to detect structural brain connectivity. For the non-clinical population with high trait anxiety level, few neuroimaging studies have focused on brain connectivity. Our previous study used tract-based spatial statistics method to compare white matter differences among young healthy individuals with low and high trait anxiety levels (8). Alterations in the thalamus–cortical circuit and some emotion-related areas are commonly reported in anxiety-related disorders (8). In the present study, three weighted networks featured by fractional anisotropy (FA), fiber number (FN), and fiber length (FL) were analyzed; and group comparisons were performed using two-sample *t*-test to explore anatomical brain connectivity changes in a healthy population with high trait anxiety levels.

We expected to find important white matter structural connections related to trait anxiety in young healthy populations with high trait anxiety levels. These findings may provide supports for establishing a neuroimaging biomarker of susceptibility to anxiety disorders to help prevent and treat the disease.

## MATERIALS AND METHODS

### Subjects

Seventy-two healthy right-handed undergraduate or postgraduate students were recruited from the Southwest University Longitudinal Imaging Multimodal, Brain Data Repository (China) ([http://fcon\\_1000.projects.nitrc.org/indi/retro/southwestuni\\_qiu\\_index.html](http://fcon_1000.projects.nitrc.org/indi/retro/southwestuni_qiu_index.html)) (9). Self-rating scores including State-Trait Anxiety Inventory (10) and Combined Raven's matrix test (CRT) (11) were measured. Subjects with trait anxiety scores exceeding 50 were classified into the high

trait anxiety (HTA) group (19 males and 19 females, trait score  $54.5 \pm 2.628$ ), and those with scores below 30 were classified into the low trait anxiety (LTA) group (14 males and 20 females, trait score  $26.177 \pm 2.516$ ) (12). The participants were matched by age ( $t = -0.567$ ,  $p = 0.572$ ) and gender ( $\chi^2 = 0.563$ ,  $p = 0.453$ ). None of the subjects presented a history of neurological or psychiatric disorders nor underwent mental health treatment and medications. All subjects conformed to the standards of MRI scanning and provided informed written consent prior to the study. The procedures of consent and experiments were approved by the Research Ethics Committee of the Brain Imaging Center of Southwest University and agreed with the standards of the Declaration of Helsinki (1989).

## Procedures

### MRI Data Acquisition

All participants were scanned using a 3.0-T Siemens Trio MRI scanner (Siemens Medical, Erlangen, Germany). Diffusion-weighted imaging (DWI) for each subject was acquired with a single-shot, spin-echo, echo-planar imaging (EPI) sequence [TR/TE = 11,000/98 ms, matrix =  $128 \times 128$ , field of view (FOV) =  $256 \times 256$  mm<sup>2</sup>, voxel size =  $2.0 \times 2.0 \times 2.0$  mm<sup>3</sup>, 60 axial slices, slice thickness = 2.0 mm, *b* value 1 = 0 s/mm<sup>2</sup>, *b* value 2 = 1,000 s/mm<sup>2</sup>] in 30 directions. The subjects were repeatedly scanned three times to increase the signal-to-noise ratio (SNR) in the DWI sequence. For each time, one *b*0 = 0 volume and 30 *b*0 = 1,000 volumes were acquired.

In addition, a magnetization-prepared rapid gradient echo (MPRAGE) sequence was used to acquire high-resolution T1-weighted anatomical images. T1-weighted structural images would be used as the templates of brain regions in the following data analysis procedure. The main parameters are as follows: repetition time = 1,900 ms, echo time = 2.52 ms, inversion time = 900 ms, flip angle = 9°, resolution matrix =  $256 \times 256$ , slices = 176, thickness = 1.0 mm, and voxel size =  $1 \times 1 \times 1$  mm<sup>3</sup>. In this study, T1 images were non-linearly transformed into the Montreal Neurological Institute (MNI) space, using the ICBM152 T1 template as a reference.

### Data Analysis

All imaging data were processed by PANDA software (13), a MATLAB toolbox that integrates MRICron (<https://www.nitrc.org/projects/mricron>), FSL (<https://fsl.fmrib.ox.ac.uk/fsl/fslwiki>), and Diffusion Toolkit (<http://www.trackvis.org/dtk/>). The flowchart of data analysis is shown in **Figure 1**. The procedure using PANDA mainly comprises data preprocessing and construction of white matter structural network.

### Image Preprocessing

In detail, the following data preprocessing steps were performed: (1) checking of image quality and converting of DICOM files into NIFTI images; (2) brain extraction and brain mask estimation; (3) cropping of images and correcting of eddy current/motion; and (4) calculation of DTI metrics (FA).

**Abbreviations:** AAL, Automated Anatomical Labeling; ACR, anterior corona radiata; BDI, Beck Depression Inventory; CRT, combined Raven's matrix test; DTI, diffusion tensor imaging; EEG, electroencephalography; FA, fractional anisotropy; FDR, false discovery rate; FL, fiber length; fMRI, functional magnetic resonance imaging; FN, fiber number; HTA, high trait anxiety; LSAS, Liebowitz Social Anxiety Scale; LTA, low trait anxiety; MNI, Montreal Neurological Institute; MRI, magnetic resonance imaging; SPIN, Social Phobia Inventory.

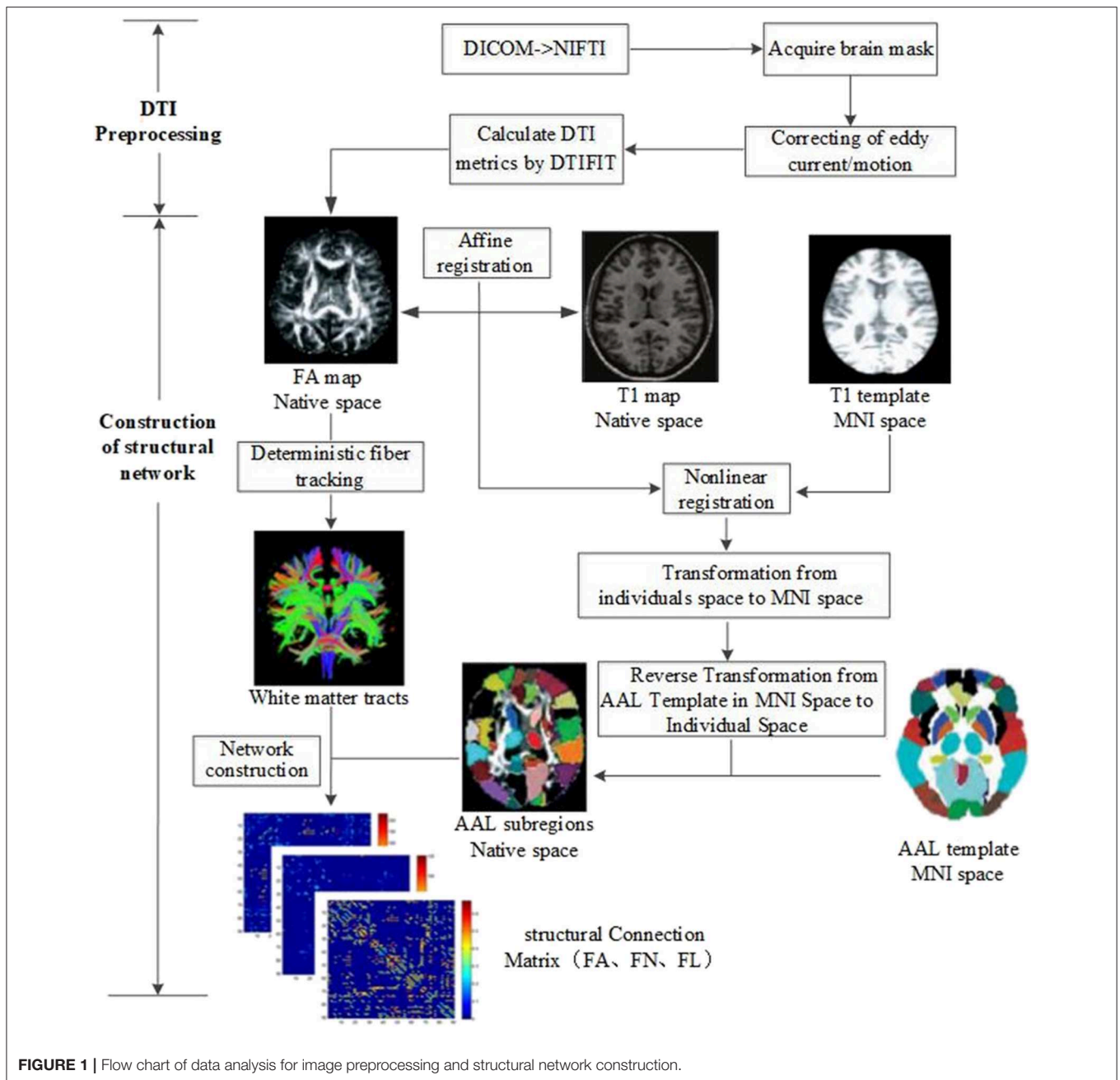


**FIGURE 1 |** Flow chart of data analysis for image preprocessing and structural network construction.

### Construction of White Matter Structural Networks

After preprocessing, white matter structural networks were constructed. (1) Affine transformation was used to match FA map and its corresponding T1 image in individual space. (2) The transformed T1 map was non-linearly registered into MNI space by T1 template. (3) Based on the above two steps, non-linear transformation from DTI individual space to MNI standard space and its inverse transformation were obtained. The Automated Anatomical Labeling (AAL) template (14) including 90 brain subregions in MNI space was registered into individual space by inverse transformation. Ninety subregions in the individual space were then segmented and labeled. (4)

White matter fibers were tracked with deterministic tracking algorithm. When  $FA < 0.2$  or direction change  $> 45^\circ$ , the white matter fiber tracking was terminated to acquire the whole brain tractography. (5) Based on the whole brain tractography, white matter structural networks could be constructed by defining FA, FN, and FL as edge weight and 90 subregions as nodes.

### Network Analysis

Graph theoretical network analysis was performed to investigate potential differences in structural network topological characteristics between HTA and LTA groups. Edges with

FN value  $<3$  and FA  $<0.2$  were excluded to eliminate the pseudoconnection or noise of the network (15). Accordingly, FA-weighted, FN-weighted, and FL-weighted matrix for the following analysis were obtained. The metrics of these networks such as global efficiency (Eg), local efficiency (Eloc), clustering coefficient (Cp), characteristic path length (Lp), and small-world property (Sigma) were calculated by GREYNA software (16). Global efficiency refers to the average inverse shortest path length, which reflects the overall efficiency of information transmission in the network. Clustering coefficient was described as the prevalence of clustered connectivity around individual nodes. The average shortest path length between all pairs of nodes in the network was called the characteristic path length (17). Local efficiency was defined as the average efficiency of the subnetwork, which described the information exchange efficiency of subnetworks. Small-world property indicated a network with high global efficiency and local efficiency (18).

In addition, edges of the three white matter connectivity matrices (FA, FN, and FL) between HTA and LTA groups were compared to identify alterations in fiber connection. The different connections were displayed using Brainnet viewer software (19).

## Statistical Analysis

Differences in structural network properties (Sigma, Eg, Eloc, Cp, and Lp) and white matter connectivities between HTA and LTA groups were assessed by two-sample *t*-test. The false discovery rate (FDR) correction for multiple comparisons was used. In addition, given that depression may influence the results, the Beck Depression Inventory (BDI) score was regarded as a covariate. The above analysis was performed by GREYNA software.

## RESULTS

### Demographic Characteristics and Behavioral Data

Demographic characteristics and behavioral data of the subjects were compared (Table 1). No significant differences in age, gender, and CRT were observed between HTA and LTA groups.

**TABLE 1** | Statistics of the demographic and behavioral data (mean and SD).

Characteristics	HTA	LTA	Test statistic	<i>p</i> -value
Gender (male/female)	38 (19/19)	34 (14/20)	$\chi^2 = 0.563$	0.453
Age (years)	20.237 $\pm$ 1.384	20.471 $\pm$ 2.078	$t = -0.567$	0.572
TAI	54.50 $\pm$ 2.628	26.177 $\pm$ 2.516	$t = 46.58$	$<0.001^*$
SAI	43.026 $\pm$ 9.356	24.882 $\pm$ 3.883	$t = 10.947$	$<0.001^*$
BDI	13.421 $\pm$ 7.366	2.294 $\pm$ 2.877	$t = 8.608$	$<0.001^*$
CRT	66.263 $\pm$ 4.157	66.088 $\pm$ 3.108	$t = 0.204$	0.839

SD, standard deviation; HTA, high trait anxiety; LTA, low trait anxiety; TAI, trait anxiety inventory; SAI, State Anxiety Inventory; BDI, Beck's Depression Inventory; CRT, combined Raven's matrix test. \* $p < 0.001$ .

## Alterations in Structural Networks

The topological properties of the three structural networks were not significantly different. However, some altered connections were detected in FA- and FN-weighted networks.

### Fractional Anisotropy-Weighted Network

Twenty-five connections featured by FA value decreased significantly in the HTA group compared with the LTA group (Table 2 and Figure 2) ( $p < 0.01$ , FDR corrected). The most different connections primarily comprised the connectivity of the left inferior orbitofrontal gyrus to the right inferior frontal gyrus (triangular), the right superior orbitofrontal gyrus to the right hippocampus, the right medial orbitofrontal gyrus to the right lenticular nucleus (putamen), the left hippocampus to the left posterior cingulate gyrus, the left thalamus, the right calcarine, the right superior temporal gyrus to the left posterior cingulate gyrus, and the right middle occipital gyrus to the right precentral gyrus ( $p < 0.001$ , FDR corrected).

### Fiber Number-Weighted Network

Twenty connections were detected to have differences ( $p < 0.01$ , FDR corrected, Table 3 and Figure 3). The most different connections primarily comprised the connectivity of the left inferior frontal gyrus (opercular) to the right inferior frontal gyrus (opercular), the right inferior frontal gyrus (triangular) to the left inferior orbitofrontal gyrus, the right superior orbitofrontal gyrus to the right hippocampus, the left hippocampus to the right calcarine and the left posterior cingulate gyrus, the right middle occipital gyrus to the right precentral gyrus, and the right superior temporal gyrus to the left posterior cingulate gyrus ( $p < 0.001$ , FDR corrected).

## DISCUSSION

To our knowledge, the investigation on white matter structural connectivity in young healthy people with high trait anxiety is limited. Our group previously used tract-based statistics method to detect the changes of white matter in young healthy populations with high trait anxiety (8). In this study, our results showed widespread abnormal connections in brain regions, but no significant difference in the network property was detected. Alterations in white matter structural connectivity were primarily located in the inter-hemispheric frontal lobe, the frontal-limbic lobe in the right hemisphere, and the frontal-temporal lobe in the ipsilateral hemisphere.

Patients with generalized anxiety disorder exhibited decreased brain signal variability in widespread regions, including the visual network, the sensorimotor network, the fronto-parietal network, the limbic system, and the thalamus (20). It should be noted that in our study, all subjects are young healthy populations. Although the HTA group has a higher trait anxiety score, they are still healthy populations, and their brains have no significant decline yet in ability their deliver global information. It may be the primary reason why the global properties of the structural brain networks did not show alterations. The abnormal connections

**TABLE 2** | Different connections in FA-weighted network.

Different connections		p-value
<b>Frontal lobe–frontal lobe</b>		
Inferior frontal gyrus (opercular)_L	Inferior frontal gyrus (opercular)_R	0.001866*
Inferior frontal gyrus (opercular)_L	Inferior frontal gyrus (triangular)_R	0.001003*
Inferior orbitofrontal gyrus_L	Inferior frontal gyrus (triangular)_R	0.000043**
<b>Frontal lobe–limbic lobe</b>		
Superior orbitofrontal gyrus_R	Hippocampus_R	0.000768**
Superior orbitofrontal gyrus_R	Lenticular nucleus, pallidum_R	0.002447*
Inferior frontal gyrus (opercular)_R	Lenticular nucleus, putamen_R	0.007135*
Supplementary motor area_R	Thalamus_L	0.008487*
Medial orbitofrontal gyrus_R	Lenticular nucleus, putamen_R	0.000383**
Paracentral lobule_R	Thalamus_R	0.006736*
<b>Frontal lobe–temporal lobe</b>		
Inferior orbitofrontal gyrus _R	Inferior temporal gyrus_R	0.002246*
Middle frontal gyrus_L	Middle temporal gyrus_L	0.007896*
Middle orbitofrontal gyrus_L	Temporal_Pole_Mid_L	0.009882*
Rectus gyrus_R	Inferior temporal gyrus_R	0.005715*
<b>Hippocampus–brain regions</b>		
Hippocampus_L	Posterior cingulate gyrus_L	0.000014**
Hippocampus_L	Thalamus_L	0.000824**
Hippocampus_L	Calcarine_R	0.000043**
ParaHippocampal gyrus_R	Middle temporal gyrus_R	0.002421*
<b>Temporal lobe–brain regions</b>		
Superior temporal gyrus_R	Posterior cingulate gyrus_L	0.000043**
Fusiform gyrus_R	Middle temporal gyrus_R	0.003185*
<b>Occipital lobe–brain regions</b>		
Middle occipital gyrus_R	Precentral gyrus_R	0.000436**
Cuneus_R	Lenticular nucleus, putamen_R	0.007813*
Calcarine_R	Inferior occipital gyrus_R	0.003976*
<b>Insula–brain regions</b>		
Insula_L	Middle occipital gyrus_L	0.009393*
Insula_R	Postcentral gyrus_R	0.005002*
Insula_R	Superior temporal gyrus_R	0.005260*

FA, fractional anisotropy; FDR, false discovery rate; L, left hemisphere; R, right hemisphere.

\* $p < 0.01$ , \*\* $p < 0.001$ ; FDR corrected.

may only influence the local information transmission a bit or even has no significant influence. Another reason may be that they are young adults aged only 20 years, and their brains will have more plasticity during their development or maturity. At the early stage, the global network properties have no such sensitivity as the biomarker to describe the brain structural change. However, the results showed that some different connections occurred in FA and FN networks. These different connections may support to elucidate our understanding of the pathological mechanism of trait anxiety in young populations.

## Thalamus-Related Connections

In our previous voxel-wise study on highly anxious population, alterations in the anterior corona radiata (ACR)–thalamus pathway have been detected, as manifested by decreased FA values in the bilateral corona radiata and anterior thalamic radiation regions. This study also showed abnormal connectivity between the left hippocampus and the thalamus. The cortical–thalamus–limbic pathway is closely associated with emotional behavior and regulation related to posttraumatic stress disorder (21). Giménez et al. found that patients with social anxiety disorder showed significant functional connections between the thalamo-cortical and fronto-striatal circuits with task induction (22). These findings suggest that thalamus-related connections may be a vulnerable marker in young healthy individuals with high anxiety.

## Temporal Lobe/Hippocampus

A large number of studies reported the importance of the hippocampus/temporal lobe for negative emotionality. Montag et al. found that four white matter tracts linking the temporal lobe/hippocampus to other brain regions were strongly correlated with trait anxiety in male participants only (23). Similarly, we demonstrated that population with high anxiety manifested significant abnormalities in 11 white matter tracts linking the temporal lobe/hippocampus to several brain regions. This study also demonstrated the abnormal connectivity of the hippocampus regions to the posterior cingulate gyrus in highly anxious populations.

## Insula

The main function of the insula is emotional processing. Baur et al. stated that the anterior insula and basolateral amygdala constitute a network that is significantly related to anxiety (6). They also supposed that the resting-state functional connection of the anterior insula to the basolateral amygdala was highly related to anxiety. Hamm et al. found that the connection of the right amygdala to the insula showed significantly increased connectivity among pediatric patients with anxiety disorders (24). Yang et al. found the abnormal functional architecture of the supramarginal gyrus network and the superior parietal gyrus network in patients with anxiety disorder (25). Dennis et al. found that the enhanced connection of the left anterior insula to the default network in healthy populations with anxiety, but connections of the parahippocampal and posterior cingulate gyrus to the default network increased in adults but not in youth (26). In addition, correlations were reported between insula activity and Liebowitz Social Anxiety Scale (LSAS) (27) or Social Phobia Inventory (SPIN) (28). We also found that the connections of the insula to the occipital and parietal lobes showed abnormality in the FA- and FN-weighted networks (the left insula to the left middle occipital gyrus, the right insula to the right postcentral gyrus in FA-weighted network, the left insula to the left superior parietal gyrus, the right insula to the right postcentral gyrus, and the left insula to left middle occipital gyrus in the FN-weighted network).

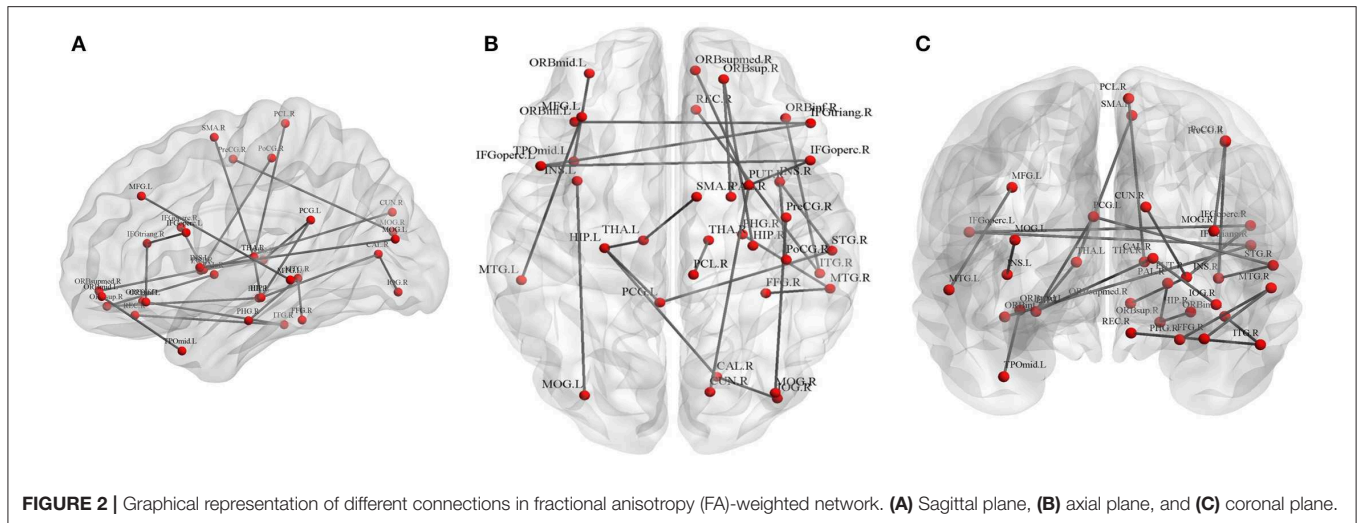


**FIGURE 2 |** Graphical representation of different connections in fractional anisotropy (FA)-weighted network. **(A)** Sagittal plane, **(B)** axial plane, and **(C)** coronal plane.

**TABLE 3 |** Different connections in FN-weighted network.

Different connections		<i>p</i> -value
<b>Frontal lobe–frontal lobe</b>		
Inferior frontal gyrus (opercular)_L	Inferior frontal gyrus (opercular)_R	0.000009**
Inferior frontal gyrus (triangular)_R	Inferior orbitofrontal gyrus _L	0.000043**
<b>Frontal lobe–limbic lobe</b>		
Superior orbitofrontal gyrus_R	Hippocampus_R	0.000025**
Superior orbitofrontal gyrus_R	Lenticular nucleus, pallidum_R	0.006374*
Paracentral lobule_R	Thalamus_R	0.005746*
Supplementary motor area_R	Lenticular nucleus, putamen_R	0.001449*
Medial orbitofrontal gyrus_R	Lenticular nucleus, putamen_R	0.005243*
<b>Hippocampus–brain regions</b>		
Hippocampus_L	Calcarine_R	0.000043**
ParaHippocampal gyrus_R	Lingual gyrus_R	0.004239*
Hippocampus_L	Posterior cingulate gyrus_L	0.000092**
Middle cingulate gyrus_R	Precuneus_L	0.006184*
<b>Insula–brain regions</b>		
Insula_L	Superior parietal gyrus_L	0.009418*
Insula_R	Postcentral gyrus_R	0.003178*
Insula_L	Middle occipital gyrus_L	0.003504*
<b>Occipital lobe–brain regions</b>		
Calcarine_L	Temporal pole:Superior temporal pole_L	0.009510*
Lingual gyrus_R	Superior orbitofrontal gyrus_R	0.006624*
Middle occipital gyrus_R	Precentral gyrus_R	0.000493**
Precuneus_L	Postcentral gyrus_L	0.002417*
<b>Temporal lobe–brain regions</b>		
Middle temporal gyrus_L	Middle frontal gyrus_L	0.008624*
Superior temporal gyrus_R	Posterior cingulate gyrus_L	0.000043**

FN, fiber number; FDR, false discovery rate; L, left hemisphere; R, right hemisphere. \**p* < 0.01, \*\**p* < 0.001, FDR corrected.

### Frontal Cortex and Limbic Areas

The orbitofrontal cortex and the prefrontal cortex located in the anterior–inferior frontal lobe play a crucial role in modulation of fear *via* the amygdala (29). Baur et al. found that the volume of the left uncinate fasciculus decreased in individuals with social anxiety disorder; this finding suggests deficient structural connectivity from high-level control areas in the orbitofrontal cortex to more basal limbic areas, such as the amygdala (30). A study on functional and structural connectivity demonstrated the relationship between trait anxiety and axial diffusivity and reported a direct pathway from the anterior insula to the basolateral amygdala (6). In our study, the observed abnormalities of several frontal lobe connections comprising connectivity linking the orbitofrontal to the limbic regions may be a trait marker in white matter structural network for young healthy individuals. In the FA- and FN-weighted network, individuals with high anxiety manifested abnormalities in the three similar pathways, including the connections of the right superior frontal gyrus (orbital part) to the limbic regions (right hippocampus, pallidum, and putamen).

Basten et al. found that some regions (inferior frontal junction areas, dorsal anterior cingulate gyrus, and left fusiform gyrus) showed significantly weaker task-specific coupling for highly anxious subjects than for those with low anxiety level (31). Kim et al. found a negative functional connectivity of amygdala–dorsal to medial prefrontal cortex in subjects with high anxiety and a positive correlation with activity at rest in subjects with low anxiety (32). Hamm et al. found that anxiety disorders showed a high connection between the left amygdala and the ventromedial prefrontal cortex and posterior cingulate cortex (24). A meta-analysis of fMRI studies investigating emotional processing in individuals who excessively worry demonstrated the convergent abnormalities at the middle frontal gyrus, the inferior frontal gyrus, and the anterior insula compared with normal controls (33). During anticipation of uncertain threat, individuals with high trait anxiety level showed significantly abnormal functional activation in the thalamus, middle temporal



## ETHICS STATEMENT

This study was carried out in accordance with the recommendations of the Declaration of Helsinki (1989) and the Research Ethics Committee of the Brain Imaging Center of Southwest University. The protocol was approved by the Research Ethics Committee of the Brain Imaging Center of Southwest University. All subjects gave written informed consent in accordance with the Declaration of Helsinki.

## AUTHOR CONTRIBUTIONS

CY and YZ made contributions to the conception, design, and analysis of DTI data and drafted the manuscript. ML interpreted and discussed the DTI data. JR and ZL made contributions to the revision of the final manuscript. All authors read and approved the final manuscript.

## REFERENCES

- Hsiao CY, Tsai HC, Chi MH, Chen KC, Chen PS, Lee IH, et al. The Association between baseline subjective anxiety rating and changes in cardiac autonomic nervous activity in response to tryptophan depletion in healthy volunteers. *Medicine*. (2016) 95:e3498. doi: 10.1097/MD.0000000000003498
- Dodd HF, Vogt J, Turkileri N, Notebaert L. Task relevance of emotional information affects anxiety-linked attention bias in visual search. *Biol Psychol*. (2017) 122:13–20. doi: 10.1016/j.biopsycho.2016.01.017
- Zhu H, Qiu C, Meng Y, Yuan M, Zhang Y, Ren Z, et al. Altered topological properties of brain networks in social anxiety disorder: a resting-state functional MRI study. *Sci Rep*. (2017) 7:43089. doi: 10.1038/srep43089
- Pacheco-Ungueti AP, Acosta A, Callejas A, Lupianez J. Attention and anxiety: different attentional functioning under state and trait anxiety. *Psychol Sci*. (2010) 21:298–304. doi: 10.1177/0956797609359624
- Liao W, Xu Q, Mantini D, Ding J, Machado-de-Sousa JP, Hallak JE, et al. Altered gray matter morphometry and resting-state functional and structural connectivity in social anxiety disorder. *Brain Res*. (2011) 1388:167–77. doi: 10.1016/j.brainres.2011.03.018
- Baur V, Hänggi J, Langer N, Jäncke L. Resting-state functional and structural connectivity within an insula-amygdala route specifically index state and trait anxiety. *Biol Psychiatry*. (2013) 73:85–92. doi: 10.1016/j.biopsycho.2012.06.003
- Xing M, Tadayonnejad R, MacNamara A, Ajilore O, Phan KL, Klump H, Leow A. EEG based functional connectivity reflects cognitive load during emotion regulation. In: *IEEE 13th International Symposium on Biomedical Imaging (ISBI)*. Chicago, IL (2016). doi: 10.1109/isbi.2016.7493380
- Lu M, Yang C, Chu T, Wu S. Cerebral white matter changes in young healthy individuals with high trait anxiety: a tract-based spatial statistics study. *Front Neurol*. (2018) 9:704. doi: 10.3389/fneur.2018.00704
- Liu W, Wei D, Chen Q, Yang W, Meng J, Wu G, et al. Longitudinal test-retest neuroimaging data from healthy young adults in southwest China. *Sci Data*. (2017) 4:170017. doi: 10.1038/sdata.2017.17
- Spielberger CD, Gorsuch RL. *Manual for the State-Trait Anxiety Inventory (form Y): ("Self-Evaluation Questionnaire")*. Palo Alto, CA: Consulting Psychologists Press, Incorporated (1983).
- Li D, Hu KD, Chen GP, Jin Y, Li M. The testing results report on the combined Raven's test in Shanghai. *Psychol Sci*. (1988) 4:27–31.
- Eden AS, Schreiber J, Anwender A, Keuper K, Laeger I, Zwanzger P, et al. Emotion regulation and trait anxiety are predicted by the microstructure of fibers between amygdala and prefrontal cortex. *J Neurosci*. (2015) 35:6020–7. doi: 10.1523/JNEUROSCI.3659-14.2015
- Cui Z, Zhong S, Xu P, Gong G, He Y. PANDA: a pipeline toolbox for analyzing brain diffusion images. *Front Hum Neurosci*. (2013) 7:42. doi: 10.3389/fnhum.2013.00042

## FUNDING

This work was supported by Beijing Nova Program (CN) (no. Z161100004916157); the National Natural Science Foundation of China (nos. 31640035, 71661167001, and 81601126); the Beijing Municipal Commission of Education (no. PXM2017\_014204\_500012); the Natural Science Foundation of Beijing (no. 4162008); and research fund for CAAE-UCB program, no. 2017010.

## ACKNOWLEDGMENTS

Thanks to the Intelligent Physiological Measurement and Clinical Translation, Beijing International Base, for their scientific and technological cooperation. Similarly, thanks also to the Southwest University Longitudinal Imaging Multimodal, Brain Data Repository (China).

- Tzourio-Mazoyer N, Landeau B, Papathanassiou D, Crivello F, Etard O, Delcroix N, et al. Automated anatomical labeling of activations in spm using a macroscopic anatomical parcellation of the MNI MRI single-subject brain. *NeuroImage*. (2002) 15:273–89. doi: 10.1006/nimg.2001.0978
- Li Y, Liu Y, Li J, Qin W, Li K, Yu C, et al. Brain anatomical network and intelligence. *NeuroImage*. (2009) 5:e1000395. doi: 10.1371/journal.pcbi.1000395
- Wang J, Wang X, Xia M, Liao X, Evans A, He Y. GREYNET: a graph theoretical network analysis toolbox for imaging connectomics. *Front Hum Neurosci*. (2015) 9:386. doi: 10.3389/fnhum.2015.00386
- Rubinov M, Sporns O. Complex network measures of brain connectivity: uses and interpretations. *NeuroImage*. (2010) 52:1059–69. doi: 10.1016/j.neuroimage.2009.10.003
- Latora V, Marchiori M. Efficient behavior of small-world networks. *Phys Rev Lett*. (2001) 87:198701. doi: 10.1103/PhysRevLett.87.198701
- Xia M, Wang J, He Y. BrainNet viewer: a network visualization tool for human brain connectomics. *PLoS ONE*. (2013) 8:e68910. doi: 10.1371/journal.pone.0068910
- Li L, Wang Y, Ye L, Chen W, Huang X, Cui Q, et al. Altered brain signal variability in patients with generalized anxiety disorder. *Front Psychiatry*. (2019) 10:84. doi: 10.3389/fpsy.2019.00084
- Schuff N, Zhang Y, Zhan W, Lenoci M, Ching C, Boreta L, et al. Patterns of altered cortical perfusion and diminished subcortical integrity in posttraumatic stress disorder: an MRI study. *NeuroImage*. (2011) 54:S62–8. doi: 10.1016/j.neuroimage.2010.05.024
- Giménez M, Pujol J, Ortiz H, Soriano-Mas C, López-Solà M, Farré M, et al. Altered brain functional connectivity in relation to perception of scrutiny in social anxiety disorder. *Psychiatr Res Neuroimaging*. (2012) 202:214–23. doi: 10.1016/j.pscychres.2011.10.008
- Montag C, Reuter M, Weber B, Markett S, Schoene-Bake JC. Individual differences in trait anxiety are associated with white matter tract integrity in the left temporal lobe in healthy males but not females. *Neuroscience*. (2012) 217:77–83. doi: 10.1016/j.neuroscience.2012.05.017
- Hamm LL, Jacobs RH, Johnson MW, Fitzgerald DA, Fitzgerald KD, Langenecker SA, et al. Aberrant amygdala functional connectivity at rest in pediatric anxiety disorders. *Biol Mood Anxiety Disord*. (2014) 4:15. doi: 10.1186/s13587-014-0015-4
- Yang F, Fan L, Zhai T, Lin Y, Wang Y, Ma J, et al. Decreased intrinsic functional connectivity in first-episode, drug-naïve adolescents with generalized anxiety disorder. *Front Hum Neurosci*. (2019) 12:539. doi: 10.3389/fnhum.2018.00539
- Dennis EL, Gotlib IH, Thompson PM, Thomason ME. Anxiety modulates insula recruitment in resting-state functional magnetic resonance imaging in youth and adults. *Brain Connectivity*. (2011) 1:245–54. doi: 10.1089/brain.2011.0030

27. Liebowitz MR. Social phobia. Modern problems of pharmacopsychiatry. (1987) 22:141–73. doi: 10.1159/000414022
28. Connor KM, Davidson JR, Churchill LE, Sherwood A, Foa E, Weisler RH. Psychometric properties of the Social Phobia Inventory (SPIN). *Br J Psychiatr.* (2000) 176:379–86. doi: 10.1192/bjp.176.4.379
29. Quirk GJ, Likhtik E, Pelletier JG, Paré D. Stimulation of medial prefrontal cortex decreases the responsiveness of central amygdala output neurons. *J Neurosci.* (2003) 23:8800–7. doi: 10.1523/JNEUROSCI.23-25-08800.2003
30. Baur V, Brühl AB, Herwig U, Eberle T, Rufer M, Delsignore A, et al. Evidence of frontotemporal structural hypoconnectivity in social anxiety disorder: a quantitative fiber tractography study. *Hum Brain Mapp.* (2011) 34:437–46. doi: 10.1002/hbm.21447
31. Basten U, Stelzel C, Fiebach CJ. Trait anxiety modulates the neural efficiency of inhibitory control. *J Cogn Neurosci.* (2011) 23:3132–45. doi: 10.1162/jocn\_a\_00003
32. Kim MJ, Gee DG, Loucks RA, Davis FC, Whalen PJ. Anxiety dissociates dorsal and ventral medial prefrontal cortex functional connectivity with the amygdala at rest. *Cereb Cortex.* (2010) 21:1667–73. doi: 10.1093/cercor/bhq237
33. Weber-Goericke F, Muehlhan M. A quantitative meta-analysis of fMRI studies investigating emotional processing in excessive worriers: application of activation likelihood estimation analysis. *J Affect Disord.* (2018) 243:348–59. doi: 10.1016/j.jad.2018.09.049
34. Geng H, Wang Y, Gu R, Luo YJ, Xu P, Huang Y, et al. Altered brain activation and connectivity during anticipation of uncertain threat in trait anxiety. *Hum Brain Mapp.* (2018) 39:3898–914. doi: 10.1002/hbm.24219
35. Du MY, Liao W, Lui S, Huang XQ, Li F, Kuang WH, Gong QY. Altered functional connectivity in the brain default-mode network of earthquake survivors persists after 2 years despite recovery from anxiety symptoms. *Soc Cogn Affect Neurosci.* (2015) 10:1497–505. doi: 10.1093/scan/nsv040
36. Makovac E, Mancini M, Fagioli S, Watson DR, Meeten F, Rae CL, et al. Network abnormalities in generalized anxiety pervade beyond the amygdala-pre-frontal cortex circuit: Insights from graph theory. *Psychiatr Res Neuroimaging.* (2018) 281:107–16. doi: 10.1016/j.psychres.2018.09.006
37. Xue S, Lee T, Guo Y. Spontaneous activity in medial orbitofrontal cortex correlates with trait anxiety in healthy male adults. *J Zhejiang Univ Sci B.* (2018) 19:643–53. doi: 10.1631/jzus.B1700481
38. Bishop S, Duncan J, Brett M, Lawrence AD. Prefrontal cortical function and anxiety: controlling attention to threat-related stimuli. *Nat Neurosci.* (2004) 7:184–8. doi: 10.1038/nn1173
39. Klumpp H, Angstadt M, Phan KL. Insula reactivity and connectivity to anterior cingulate cortex when processing threat in generalized social anxiety disorder. *Biol Psychol.* (2012) 89:273–6. doi: 10.1016/j.biopsycho.2011.10.010
40. Yang X, Liu J, Meng Y, Xia M, Cui Z, Wu X, et al. Network analysis reveals disrupted functional brain circuitry in drug-naive social anxiety disorder. *NeuroImage.* (2017) 190:213–23. doi: 10.1016/j.neuroimage.2017.12.011
41. Jacob Y, Shany O, Goldin PR, Gross JJ, Hendler T. Reappraisal of interpersonal criticism in social anxiety disorder: a brain network hierarchy perspective. *Cereb Cortex.* (2018) 29:3154–67. doi: 10.1093/cercor/bhy181
42. Brühl AB, Delsignore A, Komossa K, Weidt S. Neuroimaging in social anxiety disorder—A meta-analytic review resulting in a new neurofunctional model. *Neurosci Biobehav Rev.* (2014) 47:260–80. doi: 10.1016/j.neubiorev.2014.08.003

**Conflict of Interest:** The authors declare that the research was conducted in the absence of any commercial or financial relationships that could be construed as a potential conflict of interest.

Copyright © 2020 Yang, Zhang, Lu, Ren and Li. This is an open-access article distributed under the terms of the Creative Commons Attribution License (CC BY). The use, distribution or reproduction in other forums is permitted, provided the original author(s) and the copyright owner(s) are credited and that the original publication in this journal is cited, in accordance with accepted academic practice. No use, distribution or reproduction is permitted which does not comply with these terms.